Spectral analysis of deformed random networks

Sarika Jalan*
Max-Planck Institute for the Physics of Complex Systems, Nöthnitzerstrasse 38, D-01187 Dresden, Germany
(Received 27 March 2009; published 1 October 2009)

We study spectral behavior of sparsely connected random networks under the random matrix framework. Subnetworks without any connection among them form a network having perfect community structure. As connections among the subnetworks are introduced, the spacing distribution shows a transition from the Poisson statistics to the Gaussian orthogonal ensemble statistics of random matrix theory. The eigenvalue density distribution shows a transition to the Wigner's semicircular behavior for a completely deformed network. The range for which spectral rigidity, measured by the Dyson-Mehta Δ_3 statistics, follows the Gaussian orthogonal ensemble statistics depends upon the deformation of the network from the perfect community structure. The spacing distribution is particularly useful to track very slight deformations of the network from a perfect community structure, whereas the density distribution and the Δ_3 statistics remain identical to the undeformed network. On the other hand the Δ_3 statistics is useful for the larger deformation strengths. Finally, we analyze the spectrum of a protein-protein interaction network for *Helicobacter*, and compare the spectral behavior with those of the model networks.

DOI: 10.1103/PhysRevE.80.046101 PACS number(s): 89.75.Hc, 64.60.Cn, 89.20.−a

I. INTRODUCTION

The network concept has been gaining recognition as a fundamental tool in understanding the dynamical behavior and the response of real systems from different fields such as biology, social systems, and technological systems. Examples of biological systems include food web, nervous system, cellular metabolism, protein-protein interaction network, and gene regulatory networks; social systems include scientific collaboration, citation, and linguistic networks, and technological systems include internet and power grid [1]. Many of these networks have been shown to have universal structural properties, such as degree distribution following a power law, small diameter, large clustering coefficient, and existence of communities [1–4].

Different network models have been proposed and investigated in detail to understand systems having an underlying network structure [1–3,5]. These models concentrate to capture one or more structural properties of the networks mentioned above [1–3]. Apart from these direct measurements of structural properties, network spectra are also useful to understand various properties of the underlying system. Eigenvalues of the adjacency matrix of networks form what are called network spectra, and provide information about some basic topological properties of the underlying network [6,7]. Recently, considerable research has been done in the direction of network spectra [8,9].

In the following, we mention known results on the spectra of real world and model networks. The spectra of networks have some correspondence with the spectra of random matrices. For instance, the distribution of eigenvalues of a matrix having finite mean number p of nonzero Gaussian distributed random elements per row follows Wigner semicircular law in the limit $p \to N$, where N is the dimension of matrix [10,11]. For very small p, which corresponds to the sparse random matrix, one gets the semicircular law but with peaks at different parts of the spectrum (maximum at the eigenvalue *zero*) [12]. Recent investigations of the spectral behavior of networks, leading to matrices with entries *zero* and *one*, show that the random networks [13] follow Wigner semicircular law as well [14] with degeneracy at the eigenvalue *zero*. The small-world model networks [2] show a very complex spectral density with many sharp peaks [15], while the spectral density of the scale-free model networks [3] exhibits a triangular distribution [9,14–16]. The spectra of real world networks show remarkably different features than that of the model networks [9,15–17], and based on this observation a network construction method was proposed, which captures a peak at zero property shown by the spectra of many real world networks such as protein-protein interaction networks [17]. Recently, spacing distributions of Erdös-Rényi networks have been studied under random matrix theory (RMT) framework [18]. As connection probability decreases Ref. [18] shows a transition to the Poisson statistics. Additionally, it shows the transition to the Poisson statistics upon the deletion of nodes in the real world networks [18]. References [15,19] have shown that the spacing distributions of various model networks, namely, small-world and scale-free networks, follow the universal behavior of RMT. In contrast to [18], these works [15,19] have considered only connected networks. Furthermore, spectral rigidity such as the Δ_3 statistics, defined in Eq. (3), provides a qualitative measure of the level of randomness in networks [20]. Recently localization of eigenvectors has also been used to analyze various structural and dynamical properties of real and model networks [21].

RMT, initially proposed to explain statistical properties of nuclear spectra, has also provided successful predictions for the spectral properties of different complex systems such as disordered systems, quantum chaotic systems, and large complex atoms among these. It has been followed by numerical and experimental verifications in the last few decades [10,11]. Quantum graphs, which model the systems of

*Present address: National University of Singapore, 2 Science Drive 3, Singapore 117542; physarik@nus.edu.sg

interest in quantum chemistry, solid state physics, and transmission of waves, have also been studied under the RMT framework [22]. Recently, RMT has been shown to be useful in understanding the statistical properties of empirical cross-correlation matrices appearing in the study of multivariate time series in several problems: price fluctuations in stock market [23], electroencephalogram data [24], and variation in different atmospheric parameters [25].

In the present work we study spectral behavior of networks having community structure under the framework of RMT. The study of community structure helps to elucidate the organization of networks, and eventually could be related to the functionality of groups of nodes [4,5,26]. Regardless of the type of real world networks in terms of the degree and other structural properties [1], it is possible to distinguish communities in the whole networks [4]. However, the question of definition of the community is problematic, and usually community is assigned to the nodes which are connected densely among themselves, and are only sparsely connected with other nodes outside the community. We therefore model here community structure by sparsely connected Erdös-Rényi random networks. This simple approach considers more densely connected nodes as a definition of community, and does not pay attention to the detailed structure of the connections [5]. Recent literature is largely filled up with methods to detect communities in networks based on structural measures [27,28], whereas few works emphasize on the spectral properties such as density distribution and eigenvector analysis as well [29]. The objective of our work is not the detection of communities, rather we show the applicability of spectral methods under the RMT framework to analyze community structures in networks. Instead of paying attention to the nodes forming communities, we look for the signatures of overlapping of communities in the spectra of the corresponding adjacency matrix. We study various spectral behaviors, namely, density distribution, nearest-neighbor spacing distribution (NNSD), and spectral rigidity for deformed random networks. We find that the NNSD detects even the small mixing of communities in the network, whereas spectral rigidity probed by the Δ_3 statistics is suitable to analyze larger mixing, which is, in general, the case for real world networks. Communities are modeled by random or scale-free subnetworks, and interactions between communities are considered as random. For small interaction strength the NNSD of the network shows the transition from the Poisson to the Gaussian orthogonal ensemble (GOE) statistics. For large interactions, the Δ_3 statistics shows systematic increase in the range for which it follows GOE statistics. Finally, as an application, we study the spectral properties of a protein-protein interaction network of *Helicobacter* under the RMT framework.

II. DEFORMED NETWORKS

For an unweighted network, the adjacency matrix is defined in the following way: $A_{ij}=1$, if i and j nodes are connected and *zero* otherwise. For undirected networks, this matrix is symmetric and consequently has real eigenvalues. Random matrices corresponding to unweighted random networks have entries 0 and 1, where number of 1's in a row follows a Gaussian distribution with mean p and variance $p(1-p)$. This type of matrix is very well studied within the RMT framework [10,12]. We then turn our attention to the following structure: (1) Take m random networks with connection probability p; the spectral behavior of the matrix corresponding to each of these subnetworks (blocks) separately follows GOE statistics. The matrix corresponding to the full network would be a m block-diagonal matrix. (2) Introduce random connections among these subnetworks with probability q. This configuration leads to m block matrix, with blocks having entries *one* with portability p, and off-diagonal blocks having entries *one* with probability q. The above networks can be cast in the following form:

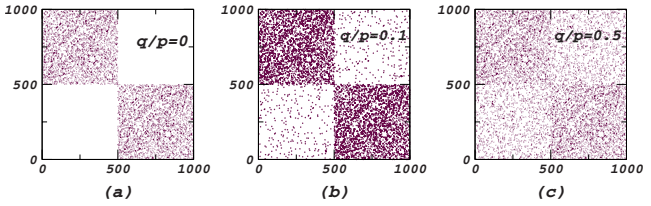

FIG. 1. (Color online) Connection matrices corresponding to $p=0.01$ and different values of q. (a) plots the connection matrix of the two subnetworks which do not have any connection between them. (b) corresponds to $q/p=0.1$, and (c) depicts the case $q/p=0.5$, when the connections between the subnetworks are as large as 50% of the connections inside.

$$A = A_0 + A_q. \tag{1}$$

A_0 is a m blocks diagonal random matrix, where each block represents one community, and the off-diagonal block matrix A_q denotes the interactions among the communities. Each block in A_q is a random matrix, which for large N has mean q and deviation $q(1-q)$. Since the nonzero values of q introduce deformation to the complete block-diagonal form, we refer A being a deformed network. This terminology is motivated by the literature on deformed random matrices [30]. Figure 1 shows the connection matrices for $m=2$ and various values of q. Figure 1(a) represents the two random subnetworks, each of size $N=500$, with the connection probability inside a subnetwork being $p=0.01$ and between the subnetworks being $q=0$. The ratio q/p, which can be considered as the relative strength of A_q and A_0, measures the deformation from the block-diagonal form of the matrix, or from the perfect structured network. The value $q/p=1$, which corresponds to equal strength of intercommunity and intracommunity connections, yields complete random network. Figure 1(b) plots the connection matrix for $q/p=0.1$, which implies that intercommunity connections are 10% of the intracommunity connections. Figure 1(c) shows the connection matrix for $q=0.005$; for this value of q, the intercommunity strength is 50% ($q/p=0.5$) of the intracommunity strength. Note that in numerical simulations we use the value of p equal to 0.01, which leads to a sparse connected random network ($N_c \sim N$) with the average degree $\langle k \rangle \sim N \times p = 5$, N_c being the number of connections in the network. Larger value of p would lead to networks with the larger average degree. Real

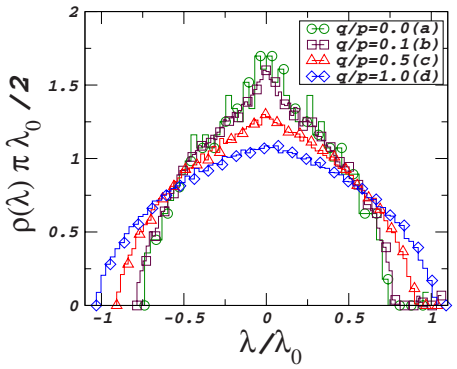

FIG. 2. (Color online) Density distribution of the two random subnetworks connecting each other with probability (a) $q=0$ and $q/p=0$; (b) $q=0.001$ and hence $q/p=0.1$; (c) $q=0.005$, hence $q/p=0.5$ and (d) $q/p=1$ which corresponds to $q=0.01$. Each block (random network) has size $N=500$. The axes are scaled in such a way that the semicircle corresponding to $q=p$ has unit radius (see text). All graphs are plotted for 20 realizations of random sets of connections among the two subnetworks.

world networks are sparse [1], and hence we chose such a small value of p.

III. NUMERICAL SIMULATION RESULTS

We denote the eigenvalues of the network by $\lambda_i, i=1,\ldots,m\times N$, where N is the size of the subnetwork, and m is the number of the subnetworks. Note that the size of each subnetwork may be different, but for simplicity we consider here equal size. Figure 2 plots the spectral density for $m=2$ block matrices having qN^2 nonzero off-diagonal entries, corresponding to the two subnetworks connected with probability q. As discussed earlier q varies from $q=0$, which corresponds to the two completely disconnected subnetworks [$A=A_0$, Fig. 1(a)], to $q=p$ leading to a single random network. The cases for $0<q\ll p$ correspond to the configurations when the initial community structure is almost preserved. Increase in the value of q leads more entries of *one* in the matrix A_q [Eq. (1)]. Finally the $q=p$ case destroys the community structure completely, and the network can be treated as one single random network. Figure 2 presents the density distribution of eigenvalues for various values of q. The eigenvalues are scaled with respect to the spectra of the network for $q/p=1$. With this scaling, the density distributions are not semicircular for values of $q<p$. As the coupling between the two blocks increases ($q>0$), the density distribution shows a transition to the semicircular form at $q=p$,

$$\rho(\lambda)=\frac{2}{\pi\lambda_0^2}\sqrt{(\lambda_0^2-\lambda^2)},$$

where λ_0 is the radius of the semicircular distribution for $q=p$ calculated from the spectra of network as $\lambda_0=(\lambda_{\max}-\lambda_{\min})/2$, $\lambda_{\max}$ and $\lambda_{\min}$ being the highest and the lowest eigenvalues. Now we turn our attention to the statistics of eigenvalue fluctuations.

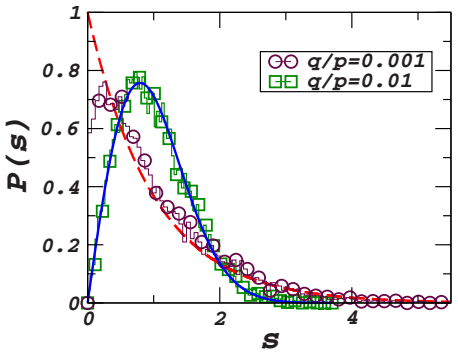

FIG. 3. (Color online) Nearest neighbor spacing distribution for the two such values of q which gives two extreme statistics. Histograms correspond to the numerical values $q=10^{-5}(q/p=0.001)$ and $q\geq 10^{-4}(q/p\geq 0.01)$. The solid and dotted curves are, respectively, Poisson and GOE predictions of RMT. The figure is plotted for an average over 20 realizations of the random set of connections between the networks.

A. Nearest-neighbor spacing distribution

In the following, we study spectral fluctuations of the networks for different values of q. In order to get universal properties of the eigenvalue fluctuations, one has to remove the spurious effects due to variations in the spectral density and to work at the constant spectral density on the average. Thereby, it is customary in RMT to unfold the eigenvalues by a transformation $\bar{\lambda}_i=\bar{N}(\lambda_i)$, where $\bar{N}(\lambda)=\int_{\lambda_{\min}}^{\lambda}\rho(\lambda')d\lambda'$ is the averaged integrated eigenvalue density [10]. Unfolding is a transformation which produces the eigenvalues with a constant average level density. Since we do not have an analytical form for $\bar{N}$, we numerically unfold the spectrum by polynomial curve fitting.

Using the unfolded eigenvalues, we calculate the NNSD $P(s)$, where $s^{(i)}=\bar{\lambda}_{i+1}-\bar{\lambda}_i$, for different q values. Figure 3 plots the spacing distribution for the two values of q, $q=0$ and $q=10^{-4}$. For such small values of q, although the density distributions remain unchanged, the NNSD shows significant changes. Spacing distributions calculated from the network spectra are fitted using Brody formula [31],

$$P_\beta(s)=As^\beta\exp(-\alpha s^{\beta+1}), \tag{2}$$

where A and α are determined by the parameter β as follows:

$$A=(1+\beta)\alpha \quad \text{and} \quad \alpha=\left[\Gamma\left(\frac{\beta+2}{\beta+1}\right)\right]^{\beta+1}.$$

Equation (2) is a semiempirical formula characterized by the single parameter β. As β goes from zero to one, the Brody formula smoothly changes from Poisson to GOE. As can be seen from Fig. 3, for $q/p\sim 0.001(q\sim 10^{-5})$, the value of the Brody parameter $\beta\sim 0.2$, which suggests that distribution is very close to the Poisson $[P(s)=\exp(-s)]$ denoted by the dotted curve in the figure. As the value of q increases, β also increases, and it is of the order of 1 for the value of $q/p\sim 0.01$ (which corresponds to the value of q as less as 10^{-4}), and becomes insensitive for a further increase in q. For larger

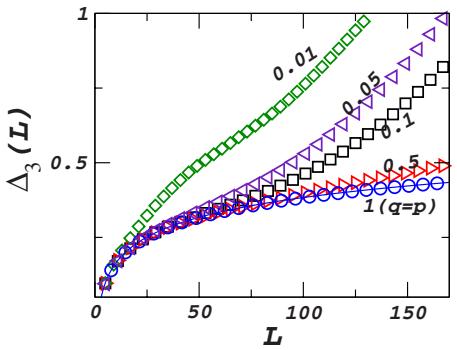

FIG. 4. (Color online) Long-range correlations among eigenvalues. Different open symbols are the numerical values of Δ_3 for various q values, and the solid curve (merged with the open circles corresponding to $q/p=1$) is the GOE prediction [Eq. (3)]. Since for $q=p$ the Δ_3 statistics of network follows the GOE prediction completely, the solid line showing GOE statistics merges with the circles showing numerical values for this q. The figure is plotted for an average over 20 realizations of the networks. Δ_3 follows the universal RMT prediction up to certain L values. The range of L for which Δ_3 follows GOE statistics increases with the ratio q/p.

values of q, we analyze the spectra using the spectral rigidity test of RMT.

B. Spectral rigidity via Δ_3 statistics

The spectral rigidity, measured by Δ_3 statistics of RMT, gives information about the long-range correlations among the eigenvalues. The Δ_3 statistics measures the least-square deviation of the spectral staircase function representing the cumulative density $N(\bar{\lambda})$ from the best straight line fitting for a finite interval L of the spectrum, i.e.,

$$\Delta_3(L;x) = \frac{1}{L}\min_{c_1,c_2} \int_x^{x+L} [N(\bar{\lambda}) - c_1\bar{\lambda} - c_2]^2 d\bar{\lambda}, \qquad (3)$$

where c_1 and c_2 are obtained from a least-square fit. Average over several choices of x gives the spectral rigidity $\Delta_3(L)$. For the uncorrelated eigenvalues, $\Delta_3(L)=L/15$, reflecting strong fluctuations around the spectral density $\rho(\lambda)$. For the GOE case, $\Delta_3(L)$ statistics is given by

$$\Delta_3(L) \sim \frac{1}{\pi^2}\ln L. \qquad (4)$$

Figure 4 plots the Δ_3 statistics for five different values of q. Various open symbols are the numerical values of Δ_3 for various q values, and the solid line (merged with the $q/p=1$ case) is the $\Delta_3(L)$ statistics for the GOE case [Eq. (4)]. As seen from Fig. 4, the $\Delta_3(L)$ statistics follows RMT predictions of GOE [Eq. (4)] up to a certain L. It has a linear behavior in semilogarithmic scale with the slope of $\sim 1/\pi^2$. The value of L for which it follows GOE statistics depends upon q. For small values of q such as $q/p=0.01$ and $q/p=0.05$, Δ_3 follows RMT prediction until very small range of $L\sim 5$ and $L\sim 20$, respectively. As q increases, the value of L for which Δ_3 follows the GOE statistics also increases. For $q/p=0.1$, it agrees with the RMT predictions of GOE behavior for $L\sim 75$, and after this value, deviation from the RMT prediction is seen. This deviation corresponds to the existence of community structure in the network. As the value of q increases, the communities have more and more random connections between them. For $q=p$ the community structure is destroyed fully, and the network is a complete random network. This fact is reflected in the Δ_3 statistics corresponding to $q/p=1$. At this value of q, it follows RMT prediction up to a very long range $L\sim 150$. After this value of L, for the network of size $N\times m=1000$ we do not have a meaningful calculation of the Δ_3 statistics [32]. For $q=0.005$ $(q/p=0.5)$ (see Fig. 1), where the strength of intercommunity is as large as $\sim 50\%$ of the intracommunity connections strength, the Δ_3 statistics correctly reflects the deviation from complete random matrices, suggesting the existence of communities in the network.

Note that we present results for each subnetwork having equal size. For subnetworks having different sizes, all the figures remain the same. The crucial quantity, which affects correlations of eigenvalues, is the variance of each block or the ratio q/p. For blocks with different sizes, but with the same q/p, similar results are obtained, except for the exact value of L in Fig. 4 for which the Δ_3 statistics follows GOE distribution, which scales with the network size [20].

IV. DEFORMED SCALE-FREE NETWORKS

In the following we consider scale-free networks as the subnetworks, and study the spectral behavior for various values of q. Again q measures the strength of the off-diagonal block matrix defining the interaction between the subnetworks. Matrix A_0 in Eq. (1), corresponding to the scale-free subnetworks, consists of two block-diagonal matrices, with entries of one in each block following a power law characteristic of the subnetwork. We use Barabási-Albert algorithm [3] to generate the scale-free subnetworks. In scale-free network the probability $P(k)$ that a node has degree k decays as a power law $P(k)\sim k^{-\gamma}$, where γ is a constant and for the type of probability law used in the simulations $\gamma=3$. Other forms for the probability law are also possible, which gives different exponent [33]. However, the results reported here are independent of the value of γ [34]. Size and average degree of the subnetworks remain the same as for the random subnetworks, i.e., $N=500$ and $\langle k\rangle=5$. The average degree $(\langle k\rangle)$ of a network can be calculated as $\langle k\rangle=2\times N_c/N$, where N_c is the number of connections and N is the size of the network. With the increase in the value of q, deformation from the network having scale-free community structure also increases. Figure 5 plots various spectral behaviors of deformed networks made of the scale-free subnetworks. Figure 5(a) plots the density distribution for the various values of q. For small values of q, the density is very different from that of the deformed random networks (Fig. 2). It has a triangular shape with a peak at zero. This is a well-known shape for sparse scale-free networks [9,15,16]. For $q/p<0.01$, when the scale-free structure of the subnetworks dominates over the random interaction between them, the eigenvalue density distribution does not show any noticeable change. But the NNSD in Fig. 5(b) suggests a possible structure in the net-

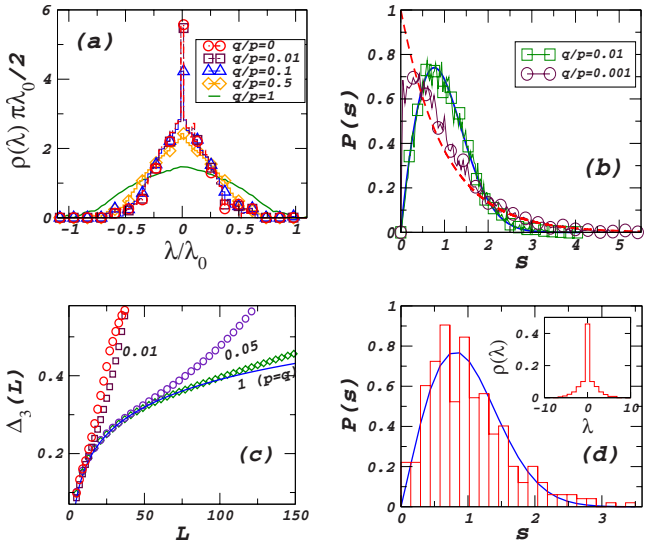

FIG. 5. (Color online) Spectral behavior of deformed scale-free networks. Subnetworks are scale-free networks of size $N=500$ and average degree $\langle k\rangle=5$. (a) plots the eigenvalue density distribution of deformed scale-free network for various values of q/p. (b) and (c) plot the NNSD and Δ_3 statistics respectively. Dashed and solid line in (b) corresponds to Poisson and GOE statistics respectively. All graphs are plotted for 20 sets of random realization of interaction networks. (d) plots the density distribution (inset), and spacing distribution for a protein-protein interaction network in *Helicobacter* as histogram and GOE statistics as solid line. This network has size $N=712$ and average degree $\langle k\rangle\sim 5$. Open circles in (c) is the Δ_3 statistics for *Helicobacter*.

work. As shown in Fig. 5(b), for $q/p=0.001$ ($q=10^{-5}$) the NNSD is close to Poisson statistics with a value of the Brody parameter $\beta\sim 0.21$. As q increases, value of the Brody parameter increases as well, becoming one for $q\sim 10^{-4}$. After this value of q, the NNSD does not provide any further insight, and we probe for long-range correlations among eigenvalues. Figure 5(c) plots the Δ_3 statistics for various values of q. It shows similar behavior as for the deformed random networks (see Fig. 4). For $q\sim 0.01$, when the network has distinguishable community structure, the value of L for which Δ_3 follows the GOE statistics (4) is as small as 25. As q is increased, L also increases, becoming ~ 150 for $q/p\sim 1$.

Figure 5(d) shows the density distribution (inset) and the spacing distribution of the protein-protein interaction network of *Helicobacter* [35]. The largest connected component of the network has dimension $N=708$ and number of connections $N_c=2789$. The average degree of this scale-free network is $\langle k\rangle\sim 4$. The density distribution has triangular form with a peak at zero. This behavior of the density distribution suggests scale-free properties of the network [9,15,16], but does not provide information of randomness or structure in the network. To get further insight, we calculate the NNSD and the spectral rigidity of the network. For this, first we unfold the eigenvalues using the procedure explained earlier. The NNSD of the network follows GOE statistics with the value of $\beta\sim 0.98$, suggesting enough random connections in the network. Further test of long-range correlations among eigenvalues shows that the Δ_3 statistics follows the GOE prediction [Eq. (4)] up to $L\sim 20$ in Fig. 5(c), and after this value deviation from the universal behavior is seen. It suggests that, though the network has enough random connections which give rise to short-range correlations among eigenvalues, it has strong community structure causing deviation of the Δ_3 statistics from the random matrix behavior after a certain range.

In the present paper we consider only the random interactions between communities. For other kind of interactions, for instance interactions among the scale-free subnetworks as considered in [5], which lead to a hierarchical scale-free network, the density distribution would show an entirely different behavior from the semicircular distribution. $p=q$ case would lead to a scale-free topology which has a triangular density distribution with peak at zero. However, spectral fluctuations would show qualitative similar behavior. For small coupling interactions among the subnetworks, the NNSD results would be same as presented here, showing a transition from Poisson to GOE statistics [20], whereas for large coupling interactions the exact range for which the Δ_3 statistics follows GOE would be different from those of the random interactions. Further detailed results of this model as well as real world networks having more complicated structures analyzed under the deformed random matrix framework would be discussed elsewhere [36].

V. CONCLUSIONS AND DISCUSSIONS

The eigenvalue density distribution of networks having two subnetworks tends toward the semicircular distribution as the random connections between the subnetworks are increased. For very small values of $q<10^{-4}$, corresponding to the very small deformation from the community structure, the density distribution does not present any noticeable changes, but the NNSD, which reflects short-range correlations among eigenvalues, show important features. For two random subnetworks, which are almost uncoupled (i.e., $q\sim 0$), the NNSD is very close to the Poisson statistics, and as q increases, it has a smooth transition to the GOE statistics. Note that this Poisson to GOE transition is found for many different systems, for example spectra of insulator-metal transition, order-chaos transition follow this Poisson-GOE transition [11]. Sade *et al.* [37] studied transition to the GOE statistics as a function of site disorder for the spectra of small-world and scale-free networks. Here, by keeping the network structure fixed, disorder at nodes is increased and depending upon the network average degree transition to GOE statistics is seen. The main difference between [37] and the study presented in this paper is the following: we track changes in the spectra with structural changes in the network architecture. As random connections among the subnetworks are increased, first there is transition for the NNSD to the GOE statistics, and this transition occurs for very small value of random connections among networks. This is the crucial and remarkably different result observed here, which suggests that very small random interaction between communities is enough to introduce short-range correlations among them, spreading the randomness in the whole network. Second, further increase in coupling among the subnetworks is

reflected by long-range correlations among eigenvalues. For this increase in the value of q, the NNSD does not give additional insight to the deformation of the network, as it remains same with the $\beta \sim 1$, so we turned our attention to the Δ_3 statistics.

The Δ_3 statistics, which measures long-range correlations among the eigenvalues, detects deformation from a network having two coupled subnetworks, to a single random network. More deformation of the network from community structure leads to a larger range of L for which Δ_3 follows the GOE statistics. Note that, for the case of subnetworks being completely random, the spacing and the Δ_3 statistics of each of them follows RMT prediction. Therefore, any deviation from GOE statistics is due to the community structure these two subnetworks form when considered as a single network.

It is interesting to note that our results resemble the behavior of deformed random matrix ensembles introduced to study the effect of isospin symmetry breaking in nuclei [30]. The qualitative behavior of the spectral density and the Δ_3 statistics of networks presented here is similar to that of deformed matrices studied in [38–40]. The analytical form of the density derived in [39] depends on a parameter α measuring the relative strength of the off-diagonal random matrices to the block-diagonal random matrices. In similar lines, for deformed networks, we can compare q/p, relative strength of off-diagonal and diagonal networks, with α. The results presented here suggest that further investigations of complex networks following similar lines as in deformed random matrices [39] would be useful to have detailed information of communities in the networks [41].

To conclude, we have studied the spectral behavior of networks having community structure, and shown that the NNSD and Δ_3 statistics capture features related to the structure in the network. We investigate the spectral properties of a real world network as well, and compare the results with those of the model networks. On the one hand, results presented in this paper advance the studies of the spectral properties of network with the community structure under the universal RMT framework; on the other hand, variations in the correlations among eigenvalues shed light on the coupling among communities. For the simulations, the community structure in network is modeled by the very simple random or scale-free subnetworks, and the interactions among these subnetworks are considered random, whereas real world networks have richer structure [5]. However, the results presented here provide a platform to investigate the community structure of networks using a well-developed theory of random matrices; the further investigations in this direction would deal with real world networks with richer and more complicated structure under the deformed random matrix framework [36,41].

ACKNOWLEDGMENTS

We acknowledge Dr. M. Hussein for useful suggestions and Dr. G. Vattay for stimulating discussions about prospective results.

[1] R. Albert and A.-L. Barabási, Rev. Mod. Phys. **74**, 47 (2002), and references therein; S. Boccaletti, V. Latora, Y. Moreno, M. Chavez, and D.-U. Hwang, Phys. Rep. **424**, 175 (2006).
[2] D. J. Watts and S. H. Strogatz, Nature (London) **440**, 393 (1998).
[3] A.-L. Barabási and R. Albert, Science **286**, 509 (1999).
[4] M. Girvan and M. E. J. Newman, Proc. Natl. Acad. Sci. U.S.A. **99**, 7821 (2002); M. E. J. Newman, Soc. Networks **27**, 39 (2005); M. E. J. Newman, Proc. Natl. Acad. Sci. U.S.A. **103**, 8577 (2006); M. J. Krawczyk, Phys. Rev. E **77**, 065701(R) (2008).
[5] E. Ravsaz *et al.*, Science **297**, 1551 (2002); R. Guimerá and L. A. N. Amaral, Nature (London) **433**, 895 (2005).
[6] D. M. Cvetković, M. Doob, and H. Sachs, *Spectra of Graphs: Theory and Applications*, 3rd ed. (Academic, New York, 1997).
[7] M. Doob, in *Handbook of Graph Theory*, edited by J. L. Gross and J. Yellen (Chapman and Hall, London, 2004).
[8] K.-I. Goh, B. Kahng, and D. Kim, Phys. Rev. E **64**, 051903 (2001); S. N. Dorogovtsev, A. V. Goltsev, J. F. F. Mendes, and A. N. Samukhin, *ibid.* **68**, 046109 (2003); E. Estrada, Europhys. Lett. **73**, 649 (2006); D. Kim and B. Kahng, Chaos **17**, 026115 (2007); H. Yang, C. Yin, G. Zhu, and B. Li, Phys. Rev. E **77**, 045101(R) (2008); G. Bianconi, e-print arXiv:0804.1744.
[9] M. A. M. de Aguiar and Y. Bar-Yam, Phys. Rev. E **71**, 016106 (2005); A. N. Samukhin, S. N. Dorogovtsev, and J. F. F. Mendes, *ibid.* **77**, 036115 (2008).
[10] M. L. Mehta, *Random Matrices*, 3rd ed. (Elsevier, Amsterdam, 2004).
[11] T. Guhr, A. Muller-Groeling, and H. A. Weidenmuller, Phys. Rep. **299**, 189 (1998).
[12] S. N. Evangelou, J. Stat. Phys. **69**, 361 (1992).
[13] P. Erdös and A. Rényi, Publ. Math., Inst. Hautes Etud. Sci. **5**, 17 (1960).
[14] I. J. Farkas, I. Derényi, A.-L. Barabási, and T. Vicsek, Phys. Rev. E **64**, 026704 (2001).
[15] J. N. Bandyopadhyay and S. Jalan, Phys. Rev. E **76**, 026109 (2007).
[16] F. Chung, L. Lu, and V. Vu, Proc. Natl. Acad. Sci. U.S.A. **100**, 6313 (2003).
[17] A. Banerjee and J. Jost, Networks Heterog. Media **3**, 395 (2008); Linear Algebr. Appl. **428**, 3015 (2008).
[18] G. Palla and G. Vattay, New J. Phys. **8**, 307 (2006).
[19] S. Jalan and J. N. Bandyopadhyay, Phys. Rev. E **76**, 046107 (2007).
[20] S. Jalan and J. N. Bandyopadhyay, EPL **87**, 048010 (2009).
[21] P. N. McGraw and M. Menzinger, Phys. Rev. E **77**, 031102 (2008); G. Zhu, H. Yang, C. Yin and B. Li, *ibid.* **77**, 066113 (2008).
[22] T. Kottos and U. Smilansky, Phys. Rev. Lett. **79**, 4794 (1997); J. Phys. A **36**, 3501 (2003).

[23] L. Laloux, P. Cizeau, J.-P. Bouchaud, and M. Potters, Phys. Rev. Lett. **83**, 1467 (1999); V. Plerou, P. Gopikrishnan, B. Rosenow, L. A. Nunes Amaral, and H. E. Stanley, *ibid.* **83**, 1471 (1999).
[24] P. Seba, Phys. Rev. Lett. **91**, 198104 (2003).
[25] M. S. Santhanam and P. K. Patra, Phys. Rev. E **64**, 016102 (2001).
[26] G. Palla, I. Derenyi, I. Farkas, and T. Vicsek, Nature (London) **435**, 814 (2005); M. E. J. Newman, Phys. Rev. E **70**, 056131 (2004); A. Arenas, A. Fernandez, and S. Gomez, New J. Phys. **10**, 053039 (2008).
[27] V. Colizza, A. Flammini, M. A. Serrano, and A. Vespignani, Nat. Phys. **2**, 110 (2006).
[28] M. E. J. Newman, Phys. Rev. E **69**, 066133 (2004); M. B. Hastings, *ibid.* **74**, 035102(R) (2006); S. Fortunato and M. Barthelemy, Proc. Natl. Acad. Sci. U.S.A. **104**, 36 (2007); P. Schuetz and A. Caflisch, Phys. Rev. E **78**, 026112 (2008).
[29] M. E. J. Newman, Phys. Rev. E **74**, 036104 (2006).
[30] N. Rosenzweig and C. E. Porter, Phys. Rev. **120**, 1698 (1960); C. E. Porter, *Statistical Theory of Spectra: Fluctuations* (Academic, New York, 1965).
[31] T. A. Brody, Lett. Nuovo Cimento **7**, 482 (1973).
[32] O. Bohigas, M.-J. Giannoni, and C. Schmidt, in *Chaotic Behaviour in Quantum Systems*, edited by G. Casati (Plenum Press, New York, 1985), p. 103.
[33] S. N. Dorogovtsev, J. F. F. Mendes, and A. N. Samukhin, Phys. Rev. Lett. **85**, 4633 (2000).
[34] The relation between the preferential attachment rule $\Pi(k) \propto k+a/m$ used in the manuscript and the degree distribution exponent γ is $\gamma=2+a/m$ [33], where a is the initial attractiveness of nodes and m is the number of connections new node makes. For the Barabási-Albert (BA) model [3], $a/m=1$, which leads to the degree distribution with $\gamma=3$. In the limit of zero initial connectivity $a=0$, all new nodes connect only the first one. This case gives $\gamma=2$, and the network would be star network, with $N-1$ nodes having *one* connection and *one* node with $N-1$ connections. The eigenvalues of this star network are $-\sqrt{N-1}, 0, \sqrt{N-1}$, which gives the spectral density with three peaks at these three values. The analysis and the comments about the spectral behavior of scale-free networks presented in Sec. IV are made for $2<\gamma\leq 3$. Most of the real world networks lie between $2<\gamma<3$ [1]. For this range the density distribution show typical triangular shape, and the tail of $\rho(\lambda)$ at large λ is related to the behavior of the degree distribution $P(k)$. In particular, as $P(k)\sim k^{-\gamma}$, $\rho(\lambda)\sim|\lambda|^{1-2\gamma}$ [8]. Nearest-neighbor spacing distribution for the individual subnetwork would show GOE statistics of RMT [19]. The spectral behavior of the combined network would show qualitative similar behavior of transition from Poisson to GOE statistics as coupling between the subnetworks is increased, only the range of $\Delta_3(L)$ statistics for which it follows GOE statistics may be different.
[35] http://pil.phys.uniroma1.it/gcalda/cosinsite/extra/data/proteins/helico.
[36] J. X. de Carvalho, S. Jalan and M. S. Hussein (unpublished).
[37] M. Sade and R. Berkovits, Phys. Rev. B **68**, 193102 (2003); M. Sade, T. Kalisky, S. Havlin, and R. Berkovits, Phys. Rev. E **72**, 066123 (2005).
[38] M. S. Hussein and M. P. Pato, Phys. Rev. Lett. **70**, 1089 (1993).
[39] A. C. Bertuola, J. X. de Carvalho, M. S. Hussein, M. P. Pato, and A. J. Sargeant, Phys. Rev. E **71**, 036117 (2005).
[40] J. X. de Carvalho, M. S. Hussein, M. P. Pato, and A. J. Sargeant, Phys. Rev. E **76**, 066212 (2007).
[41] J. X. de Carvalho, S. Jalan, and M. S. Hussein, Phys. Rev. E **79**, 056222 (2009).